Structure and Dynamics of Water in the Presence of Charged Surfactant Monolayers at the Water−CCl_4 Interface. A Molecular Dynamics Study

Karl J. Schweighofer, Ulrich Essmann,† and Max Berkowitz*

Department of Chemistry, CB3290, University of North Carolina, Chapel Hill, North Carolina 27599

Received: June 6, 1997; In Final Form: September 16, 1997[⊗]

We have performed molecular dynamics simulations of sodium dodecyl sulfate (SDS) and a model cation at the water−CCl_4 interface at a coverage of 45 Å^2/molecule. In order to isolate the effects due to the polarity of the surfactant, the model potential for the cationic surfactant is chosen to be identical to that of SDS except that the sign of all atomic charges, including counterions, are reversed. We show that the structural features of the two types of surfactant monolayers give rise to large differences in the surface potential profiles and in the overall potential difference across the water−surfactant−CCl_4 interface. In addition, we show that water in intimate contact with the ionic layer is significantly altered in terms of its dynamical properties—a decrease of up to 1 order of magnitude in the rotational correlation time for the water dipole reorientation is observed. We also show that water orientational polarization propagates well into the bulk region and that this polarization depends on the sign of the ionic surfactant.

Introduction

Interfacial systems have interested scientists for many years because of their unique physical, mechanical, and chemical properties. What delineates the interfacial region from the bulk is often unclear, largely because this distinction is a direct result of the microscopic properties of the material. Such properties are difficult to characterize, especially in the case of a buried interface—such as the interface between two immiscible liquids. Additional complications arise due to the fact that the transition from the interface into the bulk is continuous, and can occur on length scales anywhere from angstroms to nanometers. This is one reason why it is difficult to use continuum models to capture the subtlety and intrigue which makes these systems so interesting.

Spectroscopic techniques and computer simulations have helped pave the way toward a more detailed understanding of some relatively simple interfacial systems.[1−10] In this report we examine the effects of charged surfactant monolayers on a water−CCl_4 interface. We begin using sodium dodecyl sulfate (SDS) as a prototypical anionic surfactant, and then create a model cationic surfactant (CAT) which is *identical* to SDS except in the sign of the atomic charges. In this way, we are able to maintain the same surface coverage, chain length, and headgroup geometry, while focusing on the effects of transitioning from an anionic to cationic monolayer. We focus our interest on two aspects: the response of water to the layer containing the charged surfactant and "neutralizing" counterions, and in how the electrostatic behavior of the charged surfactant systems depends on the microscopic structure of the system. Using these simple models, we hope to demonstrate the connection between the electrostatic and structural properties of ionic surfactant monolayers, and the consequences on surface potential and dynamics in the interfacial region.

Methods

Model Potentials. Two molecular liquids, water and carbon tetrachloride, are present in the simulations. We use SPC water with the bond lengths and angles held constant through the use of the SHAKE algorithm.[11] The carbon tetrachloride is a fully flexible, nonpolarizable, five site model described previously.[12] The amphiphilic solute is comprised of a dodecyl sulfate hydrocarbon chain consisting of a united atom CH_3 group connected to a hydrocarbon chain of 11 united atom CH_2 sites and an esteric oxygen. The SO_4 group atoms are explicitly modeled. The dodecyl sulfate intermolecular and intramolecular potential parameters have also been described previously.[12] The model cationic surfactant is identical to dodecyl sulfate except that the sign of all charges, including the counterion, are reversed. We will call this molecule CAT (for model *cation*).

System Preparation and Equilibration. In this work we perform three separate simulations—one of the pure water−CCl_4 interface, and two with monolayer interspersed between the water and CCl_4. The water−monolayer−CCl_4 systems are comprised of 1185 water, 415 carbon tetrachloride, 36 amphiphiles, and 36 counterions in a rectangular box having X and Y dimensions of 40.249 Å and a Z dimension of 150.0 Å. The water−CCl_4 interface is in the $X-Y$ plane at $Z = 0$ Å, with water occupying the left half of the box ($Z < 0$) and CCl_4 the right half ($Z > 0$). We define the interface location as the point along Z where the water density profile $\rho(Z)$ has half its bulk value and is in contact with the CCl_4. The box is longer in the Z direction than is needed to accommodate the two liquid slabs to prevent the formation of a second water−CCl_4 interface. Instead, there are two liquid−vapor interfaces at opposite ends of the box (on the $Z < 0$ side there will be a water−vapor interface and at the $Z > 0$ side, a CCl_4 liquid−vapor interface). In addition, the Z dimension of the cell is chosen such that there is a very large separation between the liquid−vapor interfaces of the two liquids. It is also important to mention that both liquid−vapor interfaces are separated from the liquid−liquid interface by substantial regions of bulk liquid. Thus there will be no direct effect on the water−CCl_4 interface from the liquid−vapor interfaces. The pure water−CCl_4 system contains 500 water, and 152 CCl_4 molecules in a rectangular box of dimensions 24.834 Å × 24.834 Å × 110.0 Å. The Z-dependent liquid density profiles of Figure 1 provides a visual description of how the system is put together.

The SDS monolayer was prepared by first constraining the headgroups of the amphiphile to be on a cubic lattice having

† GMD-SCAI, Schloss Birlinghoven, 53754 Sankt Augustin, Germany.
⊗ Abstract published in *Advance ACS Abstracts,* November 15, 1997.

S1089-5647(97)01865-8 CCC: $14.00

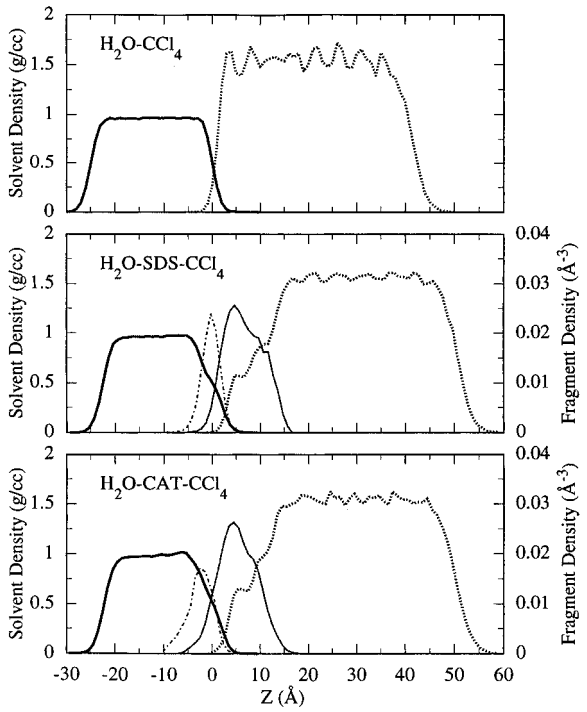

Figure 1. Solvent density profiles for the three systems calculated by binning positions into 1 Å slices along the *Z* axis. Top panel: water−CCl_4 system. Middle panel: water−SDS−CCl_4 system. Bottom panel: water−CAT−CCl_4 system. Legend: dark thick line, water; dotted thick line, CCl_4; thin solid line, hydrocarbon tail; thin dot−dash line, headgroup. The headgroup is defined as the SO_3 group and counterions, the hydrocarbon tail is defined as all carbon atoms in the amphiphile.

X−*Y* dimensions commensurate with those of the liquid−liquid simulation cell, resulting in a monolayer coverage of 45 Å^2 per molecule. The lattice was simulated, with the headgroups pinned, at 800 K for 10 ps in order to randomize the tails. The monolayer was then gradually inserted into a fully equilibrated water−CCl_4 system such that the sulfur atoms were located approximately in the center of the interfacial region with the hydrocarbon tails immersed in the organic layer. The gradual increase in the solvent−solute interaction was performed over a total time of 600 ps with periodic rescaling of the velocities to maintain a temperature of 300 K. At this point, 36 random water molecules in the interfacial region were replaced by sodium ions. The system was then equilibrated for another 200 ps using AMBER 4.1.[13] Long-range forces were calculated using particle mesh ewald (PME),[14,15] with a 9 Å cutoff. The cationic monolayer system was created by taking the fully equilibrated water−SDS−CCl_4 system and reversing the charges on all solutes. The system was equilibrated for an additional 250 ps before production runs began. Production runs, calculated at 300 K, used a time step of 1.0 fs and data collection every 20.0 fs for a total time of 0.75 ns.

Results and Discussion

The *Z*-dependent density distributions are shown in Figure 1. Each system has liquid−vapor regions at the ends of the box with a vacuum space between the liquid slabs of about 30 Å for the pure water−CCl_4 system, and 60 Å for the systems with surfactants. Oscillations in the carbon tetrachloride density distribution may be due in part to statistical fluctuations; the slightly smoother CCl_4 profiles in the larger systems bears this out. Similar fluctuations have been seen in other liquid−liquid simulations.[7,16] The average bulk densities are 0.96 g/cm^3 and 1.59 g/cm^3 for water and carbon tetrachloride, respectively. The experimental densities at 300 K are 1.0 and 1.6 g/cm^3 respectively. The point at which water has half its bulk density is at $Z = 0$ Å for all systems.

Both systems with surfactant have very similar solvent density profiles, and show a large increase in the width of the interfacial region relative to the pure water−CCl_4 system. In the water profile for the system with CAT there is also a distinguishable bump at approximately6 −5.0 Å, which occurs before the water relaxes to its bulk density. This effect is seen to a lesser degree in the SDS system. This type of deformation in water profile was observed in simulations of Na^+, F^- and Cl^- at the water−vapor interface.[17] The bulging was attributed to the fact that the anions retain part of their second solvation shell at the interface whereas Na^+ does not. In the CAT system, the Na^+ of SDS is replaced by an "Na^-" ion. The broadening of the interface itself is not unexpected since ionic surfactants tend to decrease surface tension, thus increasing the width of the interface. Such broadening has also been seen in other simulations of amphiphile monolayers at aqueous interfaces.[6,18]

The penetration of the amphiphilic head and tail regions into the water layer is slightly greater for the CAT system. In addition, a subtle change in the amphiphile distribution widths occurs upon conversion from SDS to CAT. That is, the tail distribution sharpens slightly and becomes more Gaussian; whereas the opposite trend is seen in the headgroup distribution. These changes may be attributable to some differential solubility of the head and tail regions in water, which is modified when one inverts the signs of the charges.

Experimentally it is found that for monolayers of charged surfactants on an water−vapor interface, water molecules in the interfacial region orient in response to the charged layer.[19] It has been shown that at water−vapor[20] and water-hydrocarbon[21] interfaces, water dipoles change their alignment to lie roughly in the plane of the interface. To understand how water responds to the charged surfaces, we calculate the probability distributions $P(\cos(\theta))$ and $P(\cos(\alpha))$; where θ refers to the angle the water dipole makes with the positive *Z* axis (outward normal to the water at the liquid−liquid interface). α is the angle that a water OH bond makes with the outward normal. An individual distribution is calculated for all water molecules in 1 Å slices along the interface normal, however in Figure 2 we show profiles for only three representative water layers.

The orientational profiles for water at the pure water−CCl_4 interface show many of the same characteristics seen at the water−vapor interface. Although the distributions are broad, water in the outermost layer (S1 in the top plot of Figure 2) of the interface show a preponderance to align with their dipoles directed out of the liquid at an angle of approximately 75°. From the bimodality in the OH distributions, we see that one of the hydrogens points outward from the interface and the other slightly inward (peaks at ∼0°,120°). Molecules within 1−2 molecular layers of the interface tend to be a mixture of orientations, some with their dipoles lying in the interfacial plane and one hydrogen pointing either outward, inward, or in the plane of the interface.[16,21−23] In layer S2 (3 Å deeper than S1), the dipole lies mostly within the plane of the interface and the OH distribution is very broad. The orientational distributions flatten out by −5.0 Å (layer S3) which suggests a bulklike region has been reached since all orientations become equally probable.

The S1 distribution for the SDS system is very similar to the S1 of the water−CCl_4 system, the impact of the charged region being mostly on water layers with $Z < 0$ Å. For the CAT monolayer, there are some deviations from this orientation, although the main features are preserved. In layer S2, the water

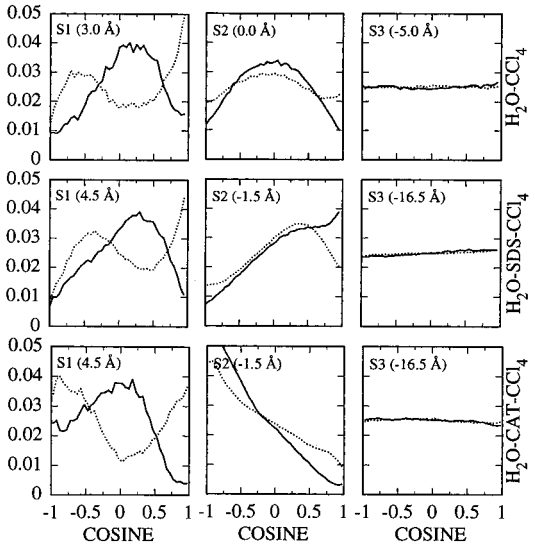

Figure 2. Dipole and OH bond angular distributions for water in 1 Å slices along the *Z* axis, and calculated as described in the text. S1, S2, and S3 describe three noncontiguous regions with distances away from the interface (located at $Z = 0$) in parentheses. Top panels: water−CCl_4 system. Middle panels: water−SDS−CCl_4 system. Bottom panels: water−CAT−CCl_4 system. Legend: solid line, water dipole; dotted line, OH bond.

shows opposite trends in orientational polarization depending on whether the surfactant is anionic or cationic. For the anionic surfactant SDS, the S2 water aligns with the dipoles pointing toward the charged layer (along the $+Z$ axis). The cationic system shows exactly the opposite alignment of water molecules in this region. These orientational polarizations have been previously proposed from experiments on charged surfactants at the water−vapor interface.[19] In the monolayer systems, the orientational ordering persists for up to 16 Å into the water lamella; indicating that although the density profiles suggest a substantial bulk region, true bulk water may be absent entirely from these systems.

Given this broad picture of water orientation and knowledge about where the charged layer is in our system, it is instructive to consider the electrostatic contributions to the electric field and potential coming from the differently charged species in the monolayer simulations. We start by calculating the *Z*-dependent charge density distributions, $Q(z)$, such that

$$Q = \int Q(Z)\,\mathrm{d}Z = 0 \tag{1a}$$

$$Q(Z) = \sum_{i=1}^{n\text{atoms}} q_i(Z) \tag{1b}$$

$$Q^{\mathrm{W}}(Z) = \sum_{i=1}^{n\text{water}} q_i(Z); \quad Q^{\mathrm{S}}(Z) = \sum_{i=1}^{n\text{solute}} q_i(Z) \tag{1c}$$

In the above equations Q refers to the total system charge, $Q(Z)$ refers to the total *Z*-dependent charge distribution, $Q^{\mathrm{W}}(Z)$ refers to the portion of $Q(Z)$ that is due to water atoms only, and $Q^{\mathrm{S}}(Z)$ refers to the portion of $Q(Z)$ that is due to solute atoms only. The appropriateness of calculating electrostatics in this way have been discussed in the literature.[24]

The total charge distribution (normalized by the permittivity of free space) for the SDS system is shown in Figure 3 on top. Remembering that the liquid−liquid interface is located at $Z = 0.0$ Å; we see that at the water liquid−vapor interface (-28.0 Å $< Z < -20.0$ Å), there is a positive followed by a negative contribution to $Q(z)$. This is due to the orientational polarization

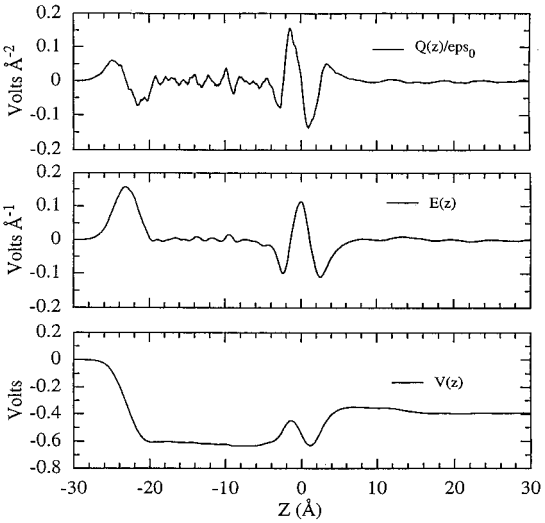

Figure 3. Total *Z*-dependent charge distribution (top), electric field (middle), and potential profile (bottom) for the water−SDS−CCl_4 system. The charge distribution $Q(z)$ was calculated by summing the individual *Z*-dependent charge distributions for all charged atoms in the system, and normalizing by the permittivity of free space. $E(z)$ was calculated by integration of $Q(z)$ along *Z*. $V(z)$ is the negative integral of $E(z)$ along *Z*.

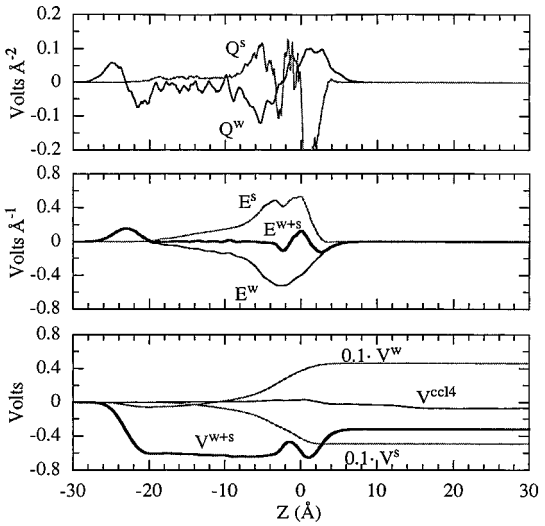

Figure 4. Contributions to $Q(z)$, $E(z)$, and $V(z)$ from water and from all solutes for the water−SDS−CCl_4 system. Q^{w}, E^{w}, and V^{w} refer to the component of $Q(z)$, $E(z)$, and $V(z)$ due to water, and similarly for solute. $E^{\mathrm{W+S}}$, and $V^{\mathrm{W+S}}$ refer to the sum of the water and solute profiles. In the bottom plot for the potential, V^{w} and V^{s} are plotted on a 1/10 scale. The potential profile for CCl_4 (V^{ccl4}) is shown in the bottom plot.

of water at the liquid−vapor interface which causes one to pass through the hydrogens first, and oxygens next, on the way into the bulk. We will not dwell-on this interface since more complete studies[25] have been done, however it provides a clear example of how to connect water orientation with the charge distributions and thus the surface potential. It is also apparent that the overall charge remains close to zero throughout the region -20.0 Å $< Z < -7.0$ Å, although there are fluctuations. Beginning at $Z = -5.0$ Å, $Q(z)$ takes on a definite structure: there appear to be four distinct layers of surface charge which alternate in sign from left to right as $-|+|-|+$ before leveling out at zero near $Z = 10.0$ Å. We can subdivide the region -5.0 Å $< Z < 10.0$ Å into five subregions using the top plot in Figure 4 to identify the major contributions to $Q(z)$ coming from the water and solute species. A summary is as follows:

3.0 Å < Z < 10.0 Å: $Q^W > 0$; $Q^s \sim 0$;
water contributes positively to $Q(z)$ which is (+).

0.0 Å < Z < 3.0 Å: $Q^W > 0$; $Q^s \ll 0$;
solute contribution dominates causing $Q(z)$ to become (−).

−2.2 Å < Z < 0.0 Å: $Q^W > 0$; $Q^s > 0$;
Q^s reverses polarity causing $Q(z)$ to become (+).

−2.8 Å < Z < −2.2 Å: $Q^W \sim 0$; $Q^s < 0$;
Q^s reverses polarity causing $Q(z)$ to become (−).

−5.0 Å < Z < −2.8 Å: $Q^W < 0$; $Q^s > 0$;
water and solute charges neutralize each other.

Thus we see that the small positive part of $Q(z)$ nearest the water−SDS−CCl_4 interface is due exclusively to water. The rest of the structure in $Q(z)$ however is a result of the structure of the monolayer headgroup region: the contributions from different parts of the amphiphile and counterions add in such a way as to produce the peaks and valleys. We have run our SDS simulations for up to 1 ns and the structure of the headgroup region remains conserved. The structure in $Q(z)$ demonstrates that simple capacitor models of charged surfactant layers need to be used with care, since they depend entirely on the microscopic structure of the interfacial region. This will be discussed in more detail later.

If we integrate the total $Q(z)$ profile we obtain the total electric field profile $E(z)$ shown in the center of Figure 3. The large field in the vicinity of the charged monolayer is quite effectively screened from the rest of the system. It also shows that water in region S1 (Z = 4.5 Å) of Figure 2 for SDS is at a place where $E(z)$ is dying off to zero, thus helping explain the similarity with the S1 water orientations for the pure water−CCl_4 system.

The negative integral of $E(z)$ yields the electrostatic potential $V(z)$ shown in the bottom plot of Figure 3. The reference potential is $V(z) = 0.0$ V in the vacuum region (Z < −30.0 Å). One sees a potential difference across the water−SDS−CCl_4 interface of approximately 200 mV. It is also clear from the bottom panel in Figure 4 that the surface potential of water V^w contributes positively to the potential across the water−SDS−CCl_4 interface, whereas that of the solute V^s contributes a nearly equal but opposite charge. The solute contribution wins out by only 300 mV (the potential difference across the water−SDS−CCl_4 due to solute and water only). This is small compared to the overall magnitudes of the water and solute surface potentials (shown on a 1/10 scale in Figure 4). The CCl_4 contribution cancels approximately 100 mV of this 300 mV difference to yield the total 200 mV reported above. In addition, the electric field contributions in the center panel of Figure 4 shows how effectively the electric field due to water E^w cancels the solute field E^s as one goes deeper into the water lamella.

Let us now turn our attention to the cationic surfactant monolayer. Quite a different picture emerges when one changes the sign of the amphiphilic monolayer and associated counterions. Figure 5 shows $Q(z)$, $E(z)$, and $V(z)$ for the CAT system. Across the water−CAT−CCl_4 interface, there is a potential drop of approximately 1.0 V; a factor of 5 larger than for SDS. The shape of the electric field and potential across the system is more or less symmetric, and the complex behavior seen in the SDS system is no longer present. We can try to understand this difference by examining the individual contributions to $Q(z)$ from Q^w and Q^s in the top panel in Figure 6.

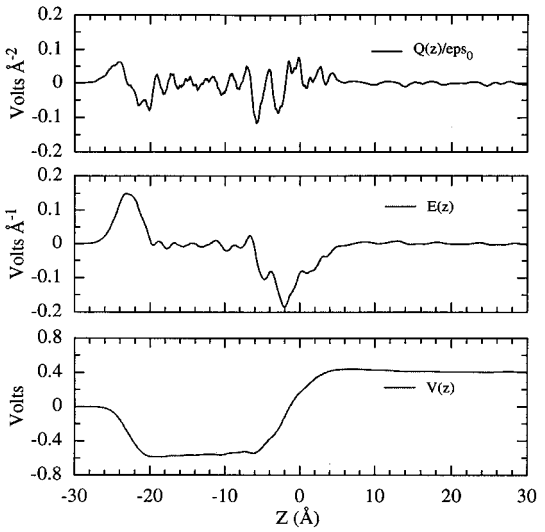

Figure 5. Total Z-dependent charge distribution (top), electric field (middle), and potential profile (bottom) for the water−CAT−CCl_4 system. This figure is the sister plot to Figure 3 and was calculated in the same fashon.

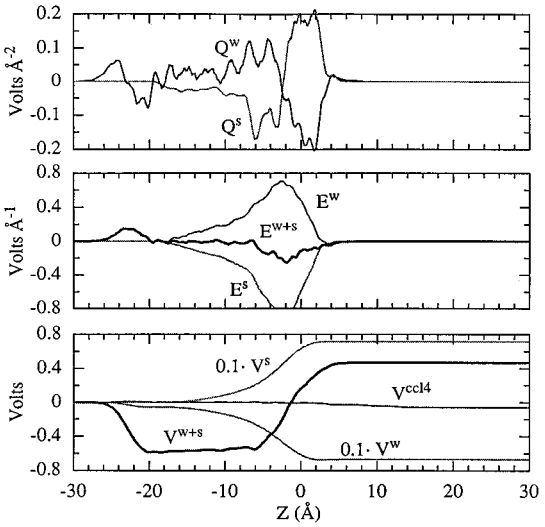

Figure 6. Contributions to $Q(z)$, $E(z)$, and $V(z)$ from water and from all solutes for the water−CAT−CCl_4 system. This figure is the sister plot to Figure 4, and the legends have the same meaning.

One apparent difference between the CAT and SDS systems is that the CAT headgroup charge distribution is more "smeared out" and is effectively quenched by the opposing water charge distribution. In addition, there is no contribution to $E(z)$ or $V(z)$ due exclusively to water (as seen in the 3.0 Å < Z < 10.0 Å region of the SDS system). The charge distribution due to water has almost the exact same shape as that of solute, but opposite in sign. The result is that the two components add in such a way as to provide a single drop in potential upon going from the nonpolar to the polar phase across the water−CAT−CCl_4 interface (bottom plot Figure 6).

Another difference arises because of a "cooperativity" effect with regards to the orientational polarization of water. Inserting an anionic surfactant into the water−CCl_4 interface enhances the tendency of water to orient with one OH pointing away from the interface. This effect propagates from the interface through many successive layers of water. For a cationic monolayer, water attempts to orient in the other direction—against it's natural tendencies. Anionic/cationic monolayers can then be viewed as providing constructive/destructive interference in the orientational polarizations of water.

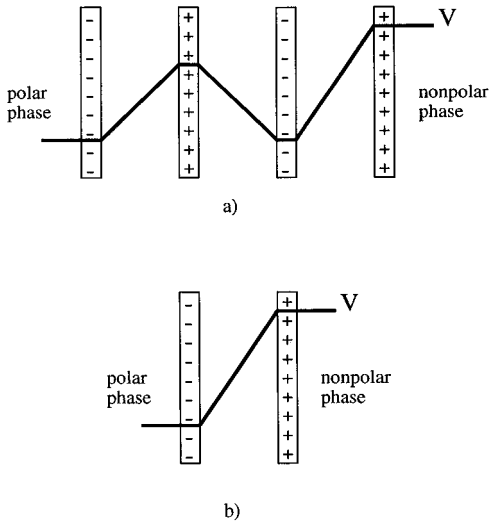

Figure 7. Capacitor models representing the change in potential across a) the water−SDS−CCl_4 interface and (b) the water−CAT−CCl_4 interface. The dark line refers to the change in potential upon crossing the interfacial region. The charge distributions are represented as charged plates.

As we mentioned previously, with care it is possible to model the changes in $V(z)$ across the surfactant interface by using a capacitor model. Such models have been popular in the past because of their simplicity; however they make the a priori assumption that the solvent, headgroups, and hydrocarbon chains can be viewed as distinct and separate layers, each giving rise to a differently charged "plate" of the capacitor.[26,27] Indeed, it is appealing to think of headgroups, hydrocarbon chains, counterions, and solvent, as individual plates in a capacitor. However, if the charged region consists of a complex mixture of contributions, which come from both solvent and solute, then it is impossible to make such distinctions. What really matters is the *total charge distribution* $Q(z)$ across the interface, which gives rise to the *total potential profile* $V(z)$. These are sensitive indicators of changes in microscopic structure in the interfacial region.

Having made this important point, we can view the water−SDS−CCl_4 interface as the three layered capacitor in Figure 7a. In this circuit, the rightmost positive plate can be attributed to water in the 3.0 Å $< Z <$ 10.0 Å region because there is negligible contribution from any other species. The other three charged "plates" are due to the fluctuations seen in $V(z)$ of Figure 3. These fluctuations are the sum from solvent and solute. The water−CAT−CCl_4 system, Figure 7b, behaves like a traditional capacitor with only two plates; and there is an inverted symmetry with respect to the center plates of the water−SDS−CCl_4 system. These differences reflect the significant changes in the environment of the charged layer upon changing the polarity of the monolayer.

Some dynamical properties of water near and far from the charged layer are shown in Figure 8. These plots are of the dipole rotational correlation functions C(t) defined as

$$C_l(t) = \langle P_l[\mathbf{r}(t + t_0)\cdot\mathbf{r}(t_0)]\rangle \qquad (2)$$

where P_l is the lth order Legendre polynomial ($l = 1$ for the dipole correlation) and $\mathbf{r}$ is the dipole vector and where the averaging is over all molecules in the specified region and over all time origins t_0 no greater than the average molecule residence time in that region. The water "far away" from the charged layer is defined as water in the region −19.0 Å $< Z <$ −14.0 Å. Water "near" the charged layer (interfacial water) is in the region $Z >$ −3.0 Å. It is apparent from both plots that the dipole rotational dynamics are much slower for interfacial water. To quantify the different reorientational behavior and to compare our results to those obtained for other interfacial systems,[16] we performed fits to the function $C(t)$ shown in Figure 8. We do this by fitting the latter part of $C(t)$ to an exponential, and calculating τ from the integral

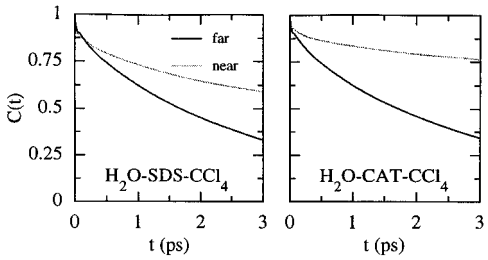

Figure 8. Water dipole rotational correlation functions, calculated as described in the text. Left plot refers to the water−SDS−CCl_4 system, right plot refers to the water−CAT−CCl_4 system. The solid lines refer to the correlation for water in the region −19 Å $< Z <$ −14.0 Å; dotted lines, the region $Z >$ −3 Å.

$$\tau = \int_0^\infty C(t)\,\mathrm{d}t = \int_0^T C(t)\,\mathrm{d}t + \int_T^\infty Ae^{-at}\,\mathrm{d}t \qquad (3)$$

where it is clear from Figure 8 that the data for $C(t)$ ends at T = 2.98 ps. We obtain for the SDS system: $\tau^{far} \sim$ 2.6 ps, $\tau^{near} \sim$ 7.8 ps. For the CAT system we get $\tau^{far} \sim$ 2.8 ps, $\tau^{near} \sim$ 24.1 ps! As a reference, the value calculated for pure SPC water at 300 K is 2.3 ps,[28] whereas experimental estimates on pure water range from 3.4 ps[28] to 6 ps.[29] For other interfacial systems, τ has been shown to increase only slightly at the interface.[30] Our results are meant to illustrate the relative degrees of mobility for water in the interfacial region as compared to the regions where the water and solute fields mostly cancel.

Summary

In performing computer simulations of anionic and cationic monolayers at the liquid−liquid interface, we demonstrate that the electrostatic properties of the system as a whole depend on the microscopic structure of the surfactant monolayer, and on the ability of water to screen the ionic charges in the interfacial region from the rest of the aqueous layers. We also show that there is a difference in structure of the anionic versus cationic monolayers, which occurs simply because of the sign of the charges on the surfactant and counterions. It is therefore possible to examine the effects of changing an anionic monolayer to a cationic one without adding complications due to variations in surface concentration, headgroup geometry, or ordering in the hydrocarbon tail region; factors which often complicate experimental studies.

Our results, in agreement with experimental results for charged surfactants at the air−water interface,[19] indicate that the orientation of water in the presence of an anionic surfactant monolayer is opposite to that of a cationic one; and extends beyond the first and even second solvation shell of the headgroups. Thus, the ordering of water is not simply attributable to chemical solvation of the headgroups; but is a result of the attempt of water to screen the field from the ionic layer. How far into the aqueous layer these fields will persist is unknown.

We also observe a "breaking of symmetry" in the potential profiles for anionic versus cationic monolayers. In the anionic monolayer, the simplified picture of a three layer capacitor represents the potential drops and increases as one moves

through the ionic layer. Upon changing the sign of the monolayer, the model reverts to a simple capacitor with a single potential difference. This asymmetry is due to the structure of the headgroup region of the SDS, and the way in which the solute and water charge distributions sum together in the ionic region. Adding in interfacial roughness due to long wavelength capillary waves (absent from the simulations because of the periodic boundary conditions) may change this picture. In any case, it demonstrates that the structure of the constituents in the region containing free charges has a significant effect on the electrostatics. This suggests that by varying components such as the size of the counterion, or the surface concentration, one might be able to "tune" the surface potential.

The reorientational dynamics of water in regions where the field is large is dramatically slowed. This is in contrast to the faster dynamics observed for water near water−vapor interfaces in the absence of surfactant. This behavior suggests a more rigid water structure, but does not demonstrate the existence of any well-defined type of structure.

Future work in this area should consider the effects of including hydrogen atoms explicitly in the surfactant model, as well as improved potentials for charged surfactants. In addition, it would be interesting to compare the behavior of ionic and nonionic surfactants at the same surface coverage.

Acknowledgment. The authors thank Michel Crowley at the Pittsburgh Supercomputer Center for a preliminary version of the AMBER/PME code. We also thank Tom Darden, Lalith Perera, Marie Messmer, and Rob Walker for helpful discussions. These calculations were performed at the North Carolina Supercomputer Center on the Crays T3D and T3E, and through a grant from the Office of Naval Research.

References and Notes

(1) Grubb, S. G.; Kim, M. W.; Raising, T.; Shen, Y. R. *Langmuir* **1988**, *4*, 452.
(2) Messmer, M.; Conboy, J. C.; Richmond, G. *J. Am. Chem. Soc.* **1995**, *117*, 8039−8040.
(3) Keller, W.; Morgner, H.; Muller, W. A. *Mol. Phys.* **1986**, *57*, 623.
(4) Sperline, R. P.; Freiser, H. *Langmuir* **1990**, *6*, 344.
(5) Wolfrum, K.; Graener, H.; Laubereau, A. *Chem. Phys. Lett.* **1993**, *213*, 41.
(6) Bocker, J.; Schlenkrich, M.; Bopp, P.; Brickmann, J. *J. Phys. Chem.* **1992**, *96*, 9915−9922.
(7) Guba, W.; Kessler, H. *J. Phys. Chem.* **1994**, *98*, 23−27.
(8) Hayoun, M.; Meyer, M.; Mareschal, M. In *Chemical Reactivity in Liquids*; Ciccotti, G., Turq, P., Eds.; Plenum: New York, 1987.
(9) Karim, O. A.; Haymet, A. D. J. *J. Chem. Phys.* **1988**, *89*, 6889.
(10) Schweighofer, K. J.; Benjamin, I. *Chem. Phys. Lett.* **1993**, *202*, 379.
(11) Ciccotti, G.; Ryckaert, J. P. *Computer Physics Reports* **1986**, *4*, 345.
(12) Schweighofer, K. J.; Essmann, U.; Berkowitz, M. *J. Phys. Chem.* **1997**, *101*, 3793−3799.
(13) Weiner, S. J.; Kollman, P. A.; Nguyen, D. T.; Case, D. A. *J. Comput. Chem.* **1986**, *7*, 230.
(14) Darden, T. A.; York, D. M.; Pedersen, L. G. *J. Chem. Phys.* **1993**, *98*, 10089−10092.
(15) Essmann, U.; Perera, L.; Berkowitz, M. L.; Darden, T.; Lee, H.; Pedersen, L. G. *J. Chem. Phys.* **1995**, *103*, 8577−8593.
(16) Benjamin, I. *J. Chem. Phys.* **1992**, *97*, 1432.
(17) Wilson, M. A.; Pohorille, A. *J. Chem. Phys.* **1991**, *95*, 6005.
(18) Tarek, M.; Tobias, D. J.; Klein, M. L. *J. Phys. Chem.* **1995**, *99*, 1393−1402.
(19) Gragson, D. E.; McCarty, B. M.; Richmond, G. L. *J. Phys. Chem.* **1996**, *100*, 14272−14275.
(20) Du, Q.; Superfine, R.; Freysz, E.; Shen, Y. R. *Phys. Rev. Lett.* **1993**, *70*, 2313.
(21) Chang, T.-M.; Dang, L. X. *J. Chem. Phys.* **1996**, *104*, 6772−6783.
(22) Linse, P. *J. Chem. Phys.* **1987**, *86*, 4177.
(23) Lee, C. Y.; McCammon, J. A.; Rossky, P. J. *J. Chem. Phys.* **1984**, *80*, 4448.
(24) Pratt, L. R. *J. Phys. Chem.* **1992**, *96*, 25−33.
(25) Wilson, M. A.; Pohorille, A.; Pratt, L. R. *J. Chem. Phys.* **1988**, *88*, 3281.
(26) Demchak, R. J.; Fort, T. Jr. *J. Colloid Interface Sci.* **1972**, *46*, 191.
(27) Petrov, J. G.; Polymeropoulos, E. E.; Mohwald, H. *J. Phys. Chem.* **1996**, *100*, 9860.
(28) Smith, P. E.; van Gunsteren, W. F. *J. Chem. Phys.* **1994**, *100*, 3169.
(29) Maroncelli, M.; Fleming, G. R. *J. Chem. Phys.* **1988**, *89*, 5044.
(30) Rossky, P. J.; Lee, S. H. *Chemica Scripta* **1989**, *29A*, 93.